AMERICAN SOCIETY FOR MICROBIOLOGY | Journal of Virology®

CELLULAR RESPONSE TO INFECTION

PD-L1 Checkpoint Inhibition Narrows the Antigen-Specific T Cell Receptor Repertoire in Chronic Lymphocytic Choriomeningitis Virus Infection

S. Klein,[a,b] D. Ghersi,[c] M. P. Manns,[a] I. Prinz,[d,e] M. Cornberg,[a,b,d,f,g] A. R. M. Kraft[a,b,g]

[a]Department of Gastroenterology, Hepatology, and Endocrinology, Hannover Medical School, Hannover, Germany
[b]Twincore, Centre for Experimental and Clinical Infection Research, Hannover, Germany
[c]School of Interdisciplinary Informatics, College of Information Science & Technology, University of Nebraska at Omaha, Omaha, Nebraska, USA
[d]Cluster of Excellence Resolving Infection Susceptibility (RESIST: EXC), Hannover Medical School, Hannover, Germany
[e]Department of Immunology, Hannover Medical School, Hannover, Germany
[f]Centre for Individualised Infection Medicine (CiiM), Hannover, Germany
[g]German Center for Infection Research (DZIF), partner site Hannover-Braunschweig, Hannover, Germany

ABSTRACT Checkpoint inhibitors are effective in restoring exhausted CD8$^+$ T cell responses in persistent viral infections or tumors. Several compounds are in clinical use for different malignancies, but trials in patients with chronic viral infections have also been conducted. In a mouse model of persistent lymphocytic choriomeningitis virus (LCMV) infection, it was shown that checkpoint inhibitor treatment increased T cell proliferation and functionality, but its influence on the antigen-specific T cell receptor (TCR) repertoire is unknown. NP396-specific CD8$^+$ T cells dominate during acute LCMV infection and are predominantly exhausted during chronic infection. Next-generation sequencing of NP396-specific TCRs showed that exhaustion corresponds with a significantly reduced NP396-specific TCR repertoire diversity: Shannon indices of 4 in immunized mice to 2.6 in persistently infected mice. Anti-PD-L1 treatment during persistent LCMV infection restored NP396-specific T cell responses and reduced viral titers. Nevertheless, anti-PD-L1-treated mice showed an even more narrowed TCR repertoire, with reduced TCR diversity compared to that of persistently infected control mice (Shannon indices of 2.1 and 2.6, respectively). Interestingly, anti-PD-L1 treatment-induced narrowing of the TCR repertoire negatively correlates with functional and physical restoration of the antigen-specific T cell response. Further, we found that private, hyperexpanded TCR clonotypes dominated the T cell response after anti-PD-L1 treatment. Although being private, these top clonotypes from anti-PD-L1-treated mice revealed a more closely related CDR3 motif than those of top clonotypes from persistently infected control mice. In conclusion, although targeting the PD-1/PD-L1 pathway reinvigorates exhausted CD8$^+$ T cells, it fails to restore T cell repertoire diversity.

IMPORTANCE Checkpoint inhibitors are effective immunotherapeutics to restore cancer- and virus-induced exhausted CD8$^+$ T cells, by enhancing the quality and survival of immune responses. Although checkpoint inhibitors are already used as therapy against various cancers, not much is known about their multifaceted impact on the exhausted CD8$^+$ T cell receptor (TCR) repertoire. This report describes for the first time the evolvement of an exhausted antigen-specific CD8$^+$ TCR repertoire under checkpoint inhibitor treatment. By using a well-established virus model, we were able to show major shifts toward oligoclonality of the CD8$^+$ TCR repertoire response against a massively exhausted lymphocytic choriomeningitis virus (LCMV) epitope. While supporting viral control in the LCMV model, oligoclonality and more private of TCR repertoires may impact future pathogenic challenges and may promote viral es-

Citation Klein S, Ghersi D, Manns MP, Prinz I, Cornberg M, Kraft ARM. 2020. PD-L1 checkpoint inhibition narrows the antigen-specific T cell receptor repertoire in chronic lymphocytic choriomeningitis virus infection. J Virol 94:e00795-20. https://doi.org/10.1128/JVI.00795-20.

Editor Stacey Schultz-Cherry, St. Jude Children's Research Hospital

Address correspondence to A. R. M. Kraft, kraft.anke@mh-hannover.de.

Received 29 April 2020
Accepted 19 June 2020
Accepted manuscript posted online 8 July 2020
Published 31 August 2020

cape. Our results may explain the ongoing problems of viral escapes, unpredictable autoimmunity, and heterogeneous responses appearing as adverse effects of checkpoint inhibitor treatments.

KEYWORDS checkpoint inhibitor, next-generation sequencing, anti-PD-L1, lymphocytic choriomeningitis virus

Immunotherapies with checkpoint inhibitors (e.g., anti-PD-1, anti-PD-L1, and anti-CTLA-4) have shown remarkable success in the treatment of a variety of tumors, and several compounds have been approved for treatment (1–5). Inhibition of the PD-1/PD-L1 pathway has also been studied consistently in persistent viral infections in animal models and *in vitro* with human samples, e.g., hepatitis B virus (HBV) and hepatitis C virus (HCV) infections (6–13). In addition, case studies and trials investigated these compounds for treatment of chronic infections such as chronic hepatitis B or C virus infection (14, 15). The current paradigm behind this treatment effect is that $CD8^+$ T cell responses in persistent viral infections or in patients with cancer are functionally impaired and express high levels of coregulatory receptors, which are called checkpoint molecules, e.g., PD-1 and CTLA-4. These so called "exhausted" T cells (16) have been described for mouse models of persistent viral infections more than 20 years ago (17). While approaching exhaustion, T cells first lose their ability to proliferate, then gamma interferon (IFN-γ) and tumor necrosis factor alpha (TNF-α) secretion becomes impaired, and, finally, cells are physically deleted (18). During this process, the checkpoint molecules (e.g., PD-1, CTLA-4, Lag-3, and Tim-3) are upregulated (19). Treatment with anti-PD-1 and anti-PD-L1 can restore functional antiviral and anti-tumor T cell responses (20–23). However, the complex biology of checkpoint pathway blockage is still largely unknown. Treatment responses are heterogeneous, and some patients develop immune-related adverse events (iAEs) (24). In this context, it became known that only a fraction of T cells are sensitive to checkpoint inhibitor therapy and restore function (25, 26), which might influence treatment outcome. In order to unravel the molecular basis of this imbalanced reinvigoration, much interest has been drawn to the question of which T cells are actually affected by the treatment. Most studies focused on phenotypic and functional markers of T cells during treatment (e.g., surface marker, functional [$cytokine^+$] T cells, and transcriptome sequencing [RNA-seq]) (26–29). However, hardly anything is known about the influence of the T cell receptor (TCR) specificity on the T cell reinvigoration and how restoration shifts the TCR repertoire. The available data are limited to analysis of the TCR repertoire of tumor-infiltrating $CD8^+$ T cells under checkpoint inhibitor treatment (30, 31). In this regard, Robert et al. could show a remodeling and broadening of the peripheral TCR repertoire of the total (not antigen-specific) $CD8^+$ T cell population in patients with melanoma, after interfering with CTLA-4 signaling (4), whereas others showed indications for a more focused TCR repertoire in a tumor environment (32, 33).

To our knowledge, nothing is known about the influence of checkpoint inhibitors on the virus-specific TCR repertoire. Therefore, we investigated the effect of the checkpoint inhibitor anti-PD-L1 on diversity, hierarchy, and specificity of the TCR repertoire of antigen-specific $CD8^+$ T cells, using the well-established lymphocytic choriomeningitis virus (LCMV) mouse model (34, 35). In this model, C57BL/6 mice either develop persistent viral infections after LCMV clone 13 (LCMV cl13) infection (2×10^6 PFU) or become immune after an acute infection with subsequent viral clearance of an LCMV Armstrong infection (5×10^4 PFU) (36). During an acute infection, the immune response is dominated by the $CD8^+$ T cell response against the epitope NP396 (37); however, this response massively exhausts during chronic infection (6). In earlier publications, Barber et al. could show that anti-PD-L1 treatment can efficiently restore this exhausted NP396-specific response (6). So far, no information about the evolving antigen-specific TCR repertoire under checkpoint inhibition is available.

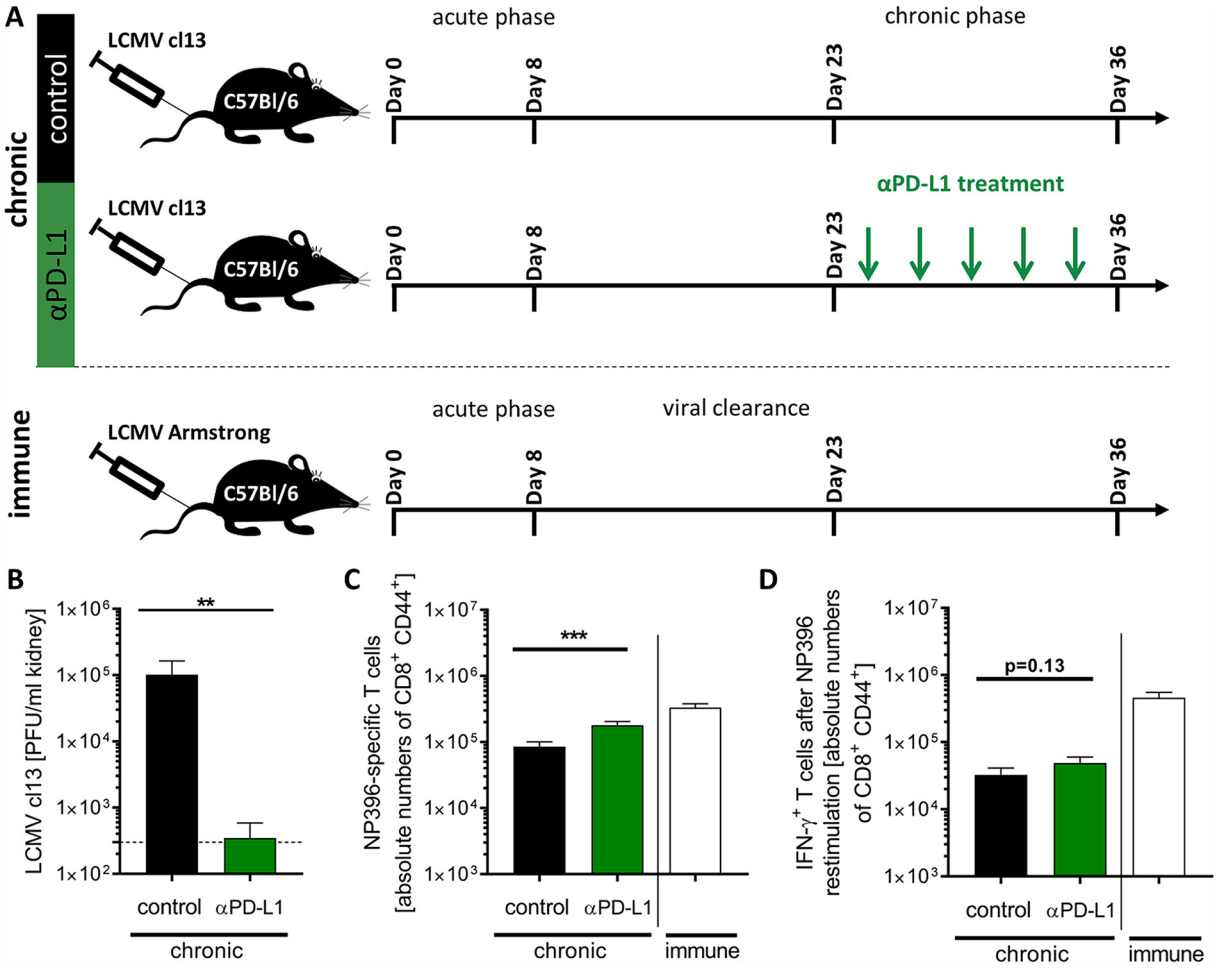

FIG 1 Checkpoint inhibitor treatment resulted in decreased LCMV titer and increased LCMV-specific T cell response. (A) Persistently LCMV cl13-infected mice were treated with anti-PD-L1 or a control. (B) Viral titers were determined in the kidney at day 36 after LCMV cl13 infection ($n = 13$ or 14). (C and D) LCMV NP396-specific T cell responses were measured by Dextramer staining ($n = 17$ to 22) (C) and by the NP396-specific IFN-γ^+ CD8$^+$ T cell response ($n = 13$ or 14) (D). As the control, NP396-specific CD8$^+$ T cell responses in LCMV-immune mice are shown ($n = 10$ to 12). Statistical comparison of both persistently infected mouse groups is depicted with asterisks. **, $P < 0.01$; ***, $P < 0.001$ (Mann-Whitney test). Results are pooled from 4 or 5 independent experiments.

RESULTS

Anti-PD-L1 treatment enhanced viral clearance and virus-specific T cell responses in persistently LCMV-infected mice. Immunocompetent C57BL/6 mice which were infected with LCMV cl13 (2×10^6 PFU) developed a persistent LCMV infection. These persistently infected mice were treated with anti-PD-L1 antibody starting at day 21 postinfection, and viral load was determined at day 36 postinfection (Fig. 1A). In line with data from Barber et al. (6), significantly reduced viral loads were found in anti-PD-L1-treated mice compared to those in control-treated mice that were persistently infected with LCMV cl13 (Fig. 1B). Moreover, anti-PD-L1 treatment resulted in a significant increase in LCMV NP396-specific CD8$^+$ T cell responses in absolute numbers (Fig. 1C) and frequencies (2.9% $\pm$ 0.37% in control-treated mice, compared to 6.2% $\pm$ 0.57% in anti-PD-L1-treated mice; $P < 0.0001$, Welch's t test), as well as a slightly increased IFN-γ^+ NP396-specific CD8$^+$ T cell response (Fig. 1D) in comparison to that in control mice. Although treatment with checkpoint inhibitors increased LCMV-specific immune responses, immune responses in LCMV-immune mice were still significantly higher than in checkpoint inhibitor-treated mice ($P < 0.001$, Kruskal-Wallis test for control and anti-PD-L1-treated mice compared to LCMV-immune mice).

Anti-PD-L1-treated mice display significantly fewer TCR-β clonotypes. To understand the impact of the reinvigoration of the exhausted NP396-specific T cells on the

TABLE 1 Sequencing raw data

Mouse	Treatment	No. of reads	No. of clonotypes	CDR3 length (main), aa	Major V chain/%
1	Control	28,333	47	14	17/70
2	Control	26,948	51	14	13-3/37
3	Control	21,298	147	15	13-2/29
4	Control	27,859	53	15	13-2/46
5	Control	3,675	49	14	17/70
6	Control	17,082	86	14	13-3/55
7	Control	24,239	54	14	13-3/27
8	Anti-PD-L1	17,153	27	15	13-3/86
9	Anti-PD-L1	18,095	16	16	13-2/72
10	Anti-PD-L1	19,598	30	14	17/45
11	Anti-PD-L1	23,363	29	14	13-2/36
12	Anti-PD-L1	28,200	51	14	13-3/76
13	Anti-PD-L1	21,810	52	14	13-3/49
14	Anti-PD-L1	2,296	9	15	3/91
15	Anti-PD-L1	12,756	46	14	19/47
16	Immune	22,564	104	14	13-3/32
17	Immune	24,885	141	14	13-3/24
18	Immune	23,952	124	14	17/25

epitope-specific T cell receptor repertoire, we determined the TCR repertoire from NP396-specific CD8$^+$ T cells in anti-PD-L1- and control-treated mice. NP396-specific CD8$^+$ T cells were isolated from spleens at day 36 postinfection, and the T cell receptor repertoire was determined using next-generation sequencing (Illumina MiSeq).

A total of 364,106 TCR-β CDR3 sequences were obtained from 18 samples, with an average of 20,228 reads per sample. While the numbers of sequencing reads generated in the different groups were not significantly different (Table 1), significantly different numbers of TCR-β clonotypes were found between the investigated groups (Fig. 2A). LCMV-immune mice had the highest number of NP396-specific CD8$^+$ T cell clonotypes (123 $\pm$ 11 clonotypes). In comparison, numbers of NP396-specific CD8$^+$ T cell clonotypes in persistently LCMV cl13-infected mice (control group) (70 $\pm$ 14 clonotypes) were significantly lower ($P < 0.05$). Treatment of persistently infected mice with anti-PD-L1 resulted in further significant reduction of NP396-specific CD8$^+$ T cell clonotypes (33 $\pm$ 6 clonotypes) compared to those in LCMV cl13-infected mice (controls) (Fig. 2A). Next, we calculated the diversity of these TCR-β repertoires, which was strongly influenced by the TCR-β clonotype numbers. By covering also the evenness of the repertoire in diversity analysis, the difference between immune and persistently infected mice became even more obvious. Furthermore, the reduced clonotype numbers

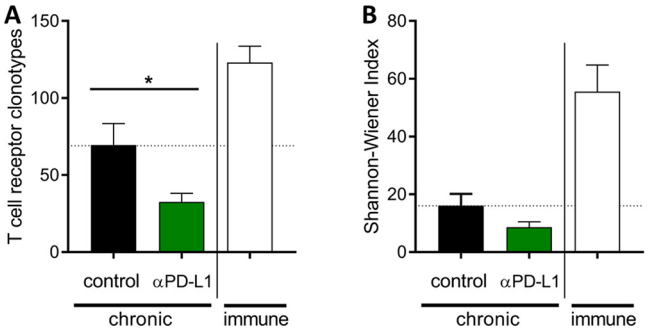

FIG 2 Severely reduced number of NP396-specific TCR-β clonotype specificities after anti-PD-L1 treatment. Persistently LCMV cl13-infected mice were treated with anti-PD-L1 ($n = 8$) or a control ($n = 7$). As a control, LCMV-immune mice were used ($n = 3$). Sequencing of NP396-specific TCR-β clonotypes in all groups was performed with an Illumina MiSeq. The number of NP396-specific TCR-β clonotypes (A) and the diversity, calculated by the Shannon-Wiener index (B), of the NP396-specific T cell receptor repertoires are depicted. *, $P < 0.05$ (Welch's t test). Results are pooled from 3 independent experiments.

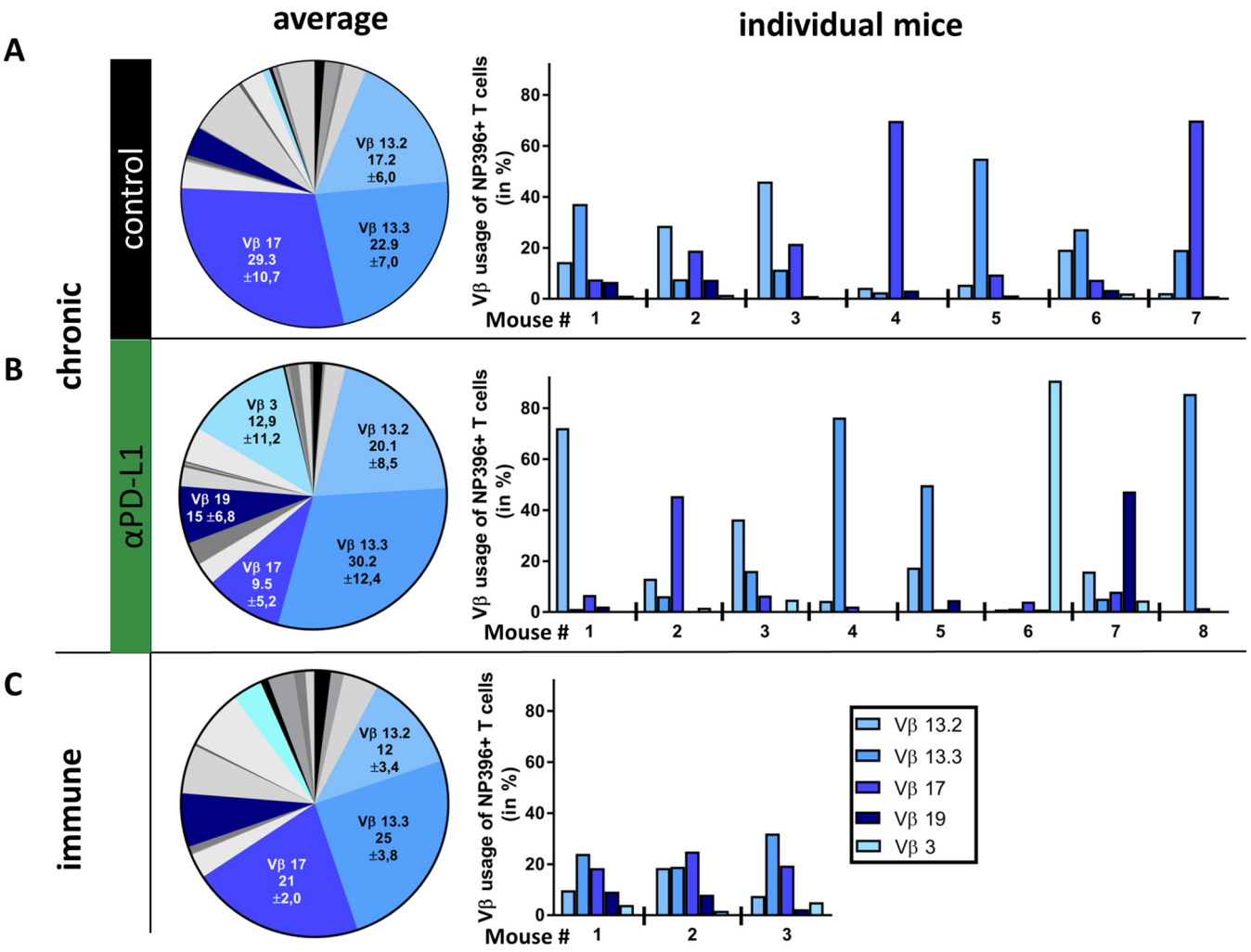

FIG 3 Three major Vβ chains dominate the immune response against NP396, using private preferences. TCR Vβ chain usage of NP396-specific TCR-β clonotypes in control-treated (A) and anti-PD-L1-treated (B) persistently LCMV cl13-infected mice, as well as LCMV-immune C57BL/6 mice (C), is depicted as mean percentage ± SEM of each individual group (circular plots). For each group, individual mice are depicted by showing five representative TCR Vβ chain usages. Results are pooled from 3 independent experiments.

in anti-PD-L1-treated mice compared to those in controls translated also to an overall reduced diversity, as calculated with the Shannon-Wiener index (Fig. 2B).

Our data showed a significant narrowing in the number of NP396-specific CD8$^+$ T cell receptor clonotypes in persistent viral infection. Treatment with anti-PD-L1 even resulted in a more oligoclonal NP396-specific T cell response.

The LCMV-specific T cell response was dominated by three public Vβ chains but displayed a high degree of privacy. So far, our study could confirm a strong reinvigoration of the NP396-specific CD8$^+$ T cell responses by anti-PD-L1 treatment but revealed also a firm reduction of TCR-β clonotype numbers within these responses. Whether this reduction correlated also with a reduction of the used Vβ chains was investigated next. A strong focusing of the TCR Vβ usage can be seen as a marker for efficient clonal expansion but also as a negative evolvement of an immune response, due to its susceptibility to viral immune evasion.

Our data revealed that three public Vβ chains (Vβ13-2, Vβ13-3, and Vβ17) dominated the immune response against NP396 in all three groups, being used in roughly two-thirds of all TCR-β clonotypes detected (Fig. 3). Overall means in the pie chart in Fig. 3 show that the average Vβ chain usage did not undergo major changes due to treatment. There was only one exception, Vβ3, which was detected strongly in only one anti-PD-L1-treated mouse, resulting in an appearance of Vβ3 at more than 12% in the

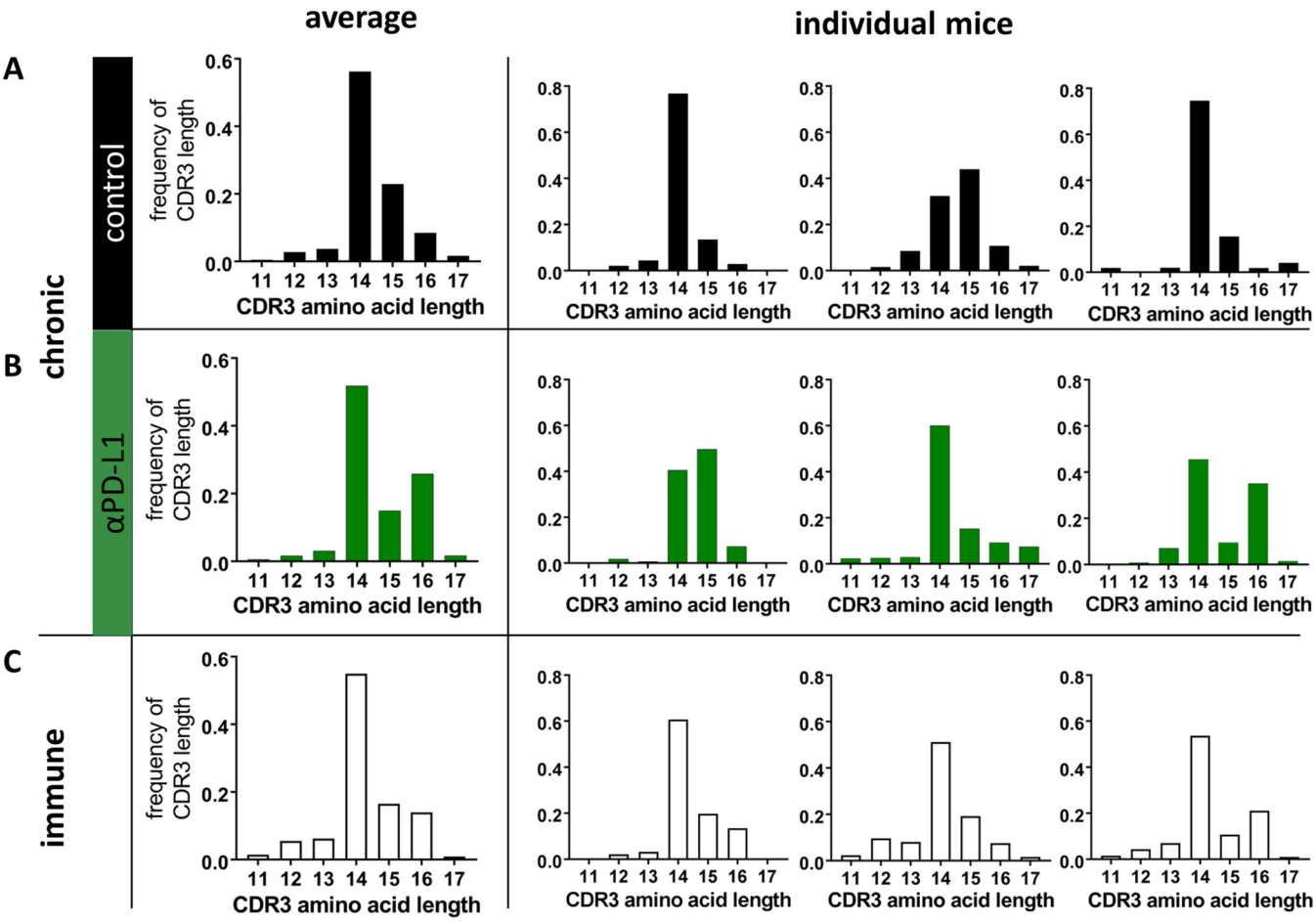

FIG 4 NP396-specific T cells predominantly reveal 14-aa CDR3 sequences. CDR3 nucleotide length in control-treated (A) and anti-PD-L1-treated (B) persistently LCMV cl13-infected C57BL/6 mice, as well as LCMV-immune C57BL/6 mice (C), is depicted as frequency of all clonotypes. The left portion defines the overall CDR3 length as an average of the respective group. Additionally, three representative mice are depicted (right portion), revealing individual patterns. Results are pooled from 3 independent experiments.

overall anti-PD-L1 group average. Moreover, looking at the individual Vβ chain usage patterns between our investigated groups, an individual Vβ chain usage was determined, called private specificity (38). Whereas immune mice showed a balanced Vβ chain usage over the five representative Vβ chains (Fig. 3C), persistently infected mice revealed a more focused usage toward one immunodominant Vβ chain (Fig. 3A). For example, whereas mouse 3 showed strong usage of Vβ13.2 and only minor usage of Vβ13.3, this pattern was reversed in mouse 5 (Fig. 3A). This effect became even more pronounced in anti-PD-L1-treated mice, in which one Vβ chain dominated the immune response (Fig. 3B). However, since the Vβ chains differed between mice overall, comparable averages of Vβ chain usages appeared in all groups.

We conclude that although no systemic focusing toward certain Vβ chains was seen in average Vβ chain usage, the individual TCR repertoires of individual mice developed privately toward a focused usage during persistent infections, which became even more pronounced under anti-PD-L1 treatment.

Impact of anti-PD-L1 treatment on the length of the NP396-specific TCR-β CDR3. Earlier reports have shown that the average CDR3 length of T cells is modulated by antigen experience and antiviral treatment (39–41). Therefore, we investigated possible changes in the CDR3 length in our study.

LCMV cl13-infected mice without anti-PD-L1 treatment as well as LCMV-immune mice showed a Gaussian distribution (Fig. 4A and C). CDR3 sequences are dominantly 14 amino acids (aa) long in their individual NP396-specific TCR-β repertoires,

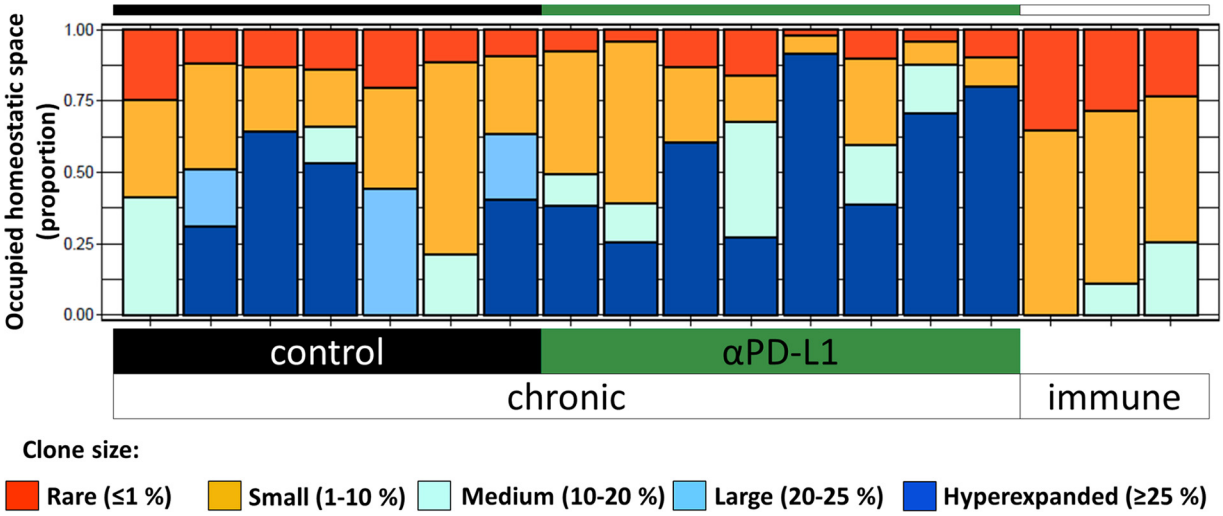

FIG 5 Hyperexpanded TCR-β clonotypes dominate the NP396-specific immune response after anti-PD-L1 treatment. NP396-specific TCR-β clonotypes from control-treated and anti-PD-L1-treated persistently LCMV cl13-infected, as well as LCMV-immune, C57BL/6 mice are depicted for each individual mouse. Clonotypes were grouped in regard to their individual relative frequency: sum of relative frequency of all hyperexpanded clonotypes (defined as ≥25% in relative frequency) is depicted in dark blue, "large" clonotypes (20 to 25%) in light blue, "medium" clonotypes (10 to 20%) in turquoise, "small" clonotypes (1 to 10%) in orange, and "rare" clonotypes (≤1%) in red. Results are pooled from 3 independent experiments.

whereas in anti-PD-L1-treated mice, either 15- or 16-aa-long sequences became codominant with the 14-aa-long CDR3s (Fig. 4B). In summary, anti-PD-L1-treated mice showed a slightly higher percentage of longer (16 aa) CDR3 sequences than controls. As shown for the Vβ chain usage, individual CDR3 length patterns seem to be very private.

Anti-PD-L1 induced a hyperexpanded and oligoclonal TCR repertoire which negatively correlated with NP396-specific responses. We could show that the NP396-specific TCR repertoire became less diverse due to anti-PD-L1 treatment. Further, Vβ chain usage showed that the TCR repertoire of each mouse posttreatment was strongly focused on one Vβ chain in anti-PD-L1-treated mice. In order to analyze the basis of the diversity loss, the TCR repertoire was depicted in a clonal space homeostasis plot (Fig. 5), showing the occupancy of clonotypes in frequency of the overall TCR repertoire, grouped by abundance. This displayed an obvious difference between immune and persistently infected mice. Large and hyperexpanded clonotypes appeared only in the latter ones. In contrast, a reduction of the rare clonotypes (red in Fig. 5) was visible. Especially "hyperexpanded" clonotypes, which make up ≥25% of the TCR repertoire, were found in all anti-PD-L1-treated mice but in only 57% of control-treated mice (Fig. 5). Such hyperexpansion and subsequent reduction of rare clonotypes could be the reason for the reduced diversity in persistently infected mice. Likewise, increased hyperexpansion in anti-PD-L1-treated mice could be the reason for an even stronger reduction of clonotype numbers in this group.

Next we asked whether the strong hyperexpansion and subsequent reduction of rare clonotypes after anti-PD-L1 treatment were associated with increased $CD8^+$ T cell responses (Fig. 1). A strong indication for this could be found by a correlation between clonotype numbers and the $NP396^+$ $CD8^+$ T cells as well as IFN-γ^+ NP396-specific $CD8^+$ T cell responses. The lower the number of clonotypes, the stronger was the immune response against NP396 in mice treated with anti-PD-L1 (Fig. 6B). This correlation was not detectable in control-treated mice (Fig. 6A).

Anti-PD-L1 strengthens the expansion of specific motifs, inducing more similar CDR3 specificities. Anti-PD-L1 therapy induced hyperexpansion of a few NP396-specific T cells, which raised the question of whether these specific clonotypes follow a certain pattern. It could be suggested that NP396-specific T cells need a TCR with a certain CDR3 motif in order to hyperexpand in response to anti-PD-L1 treatment. To

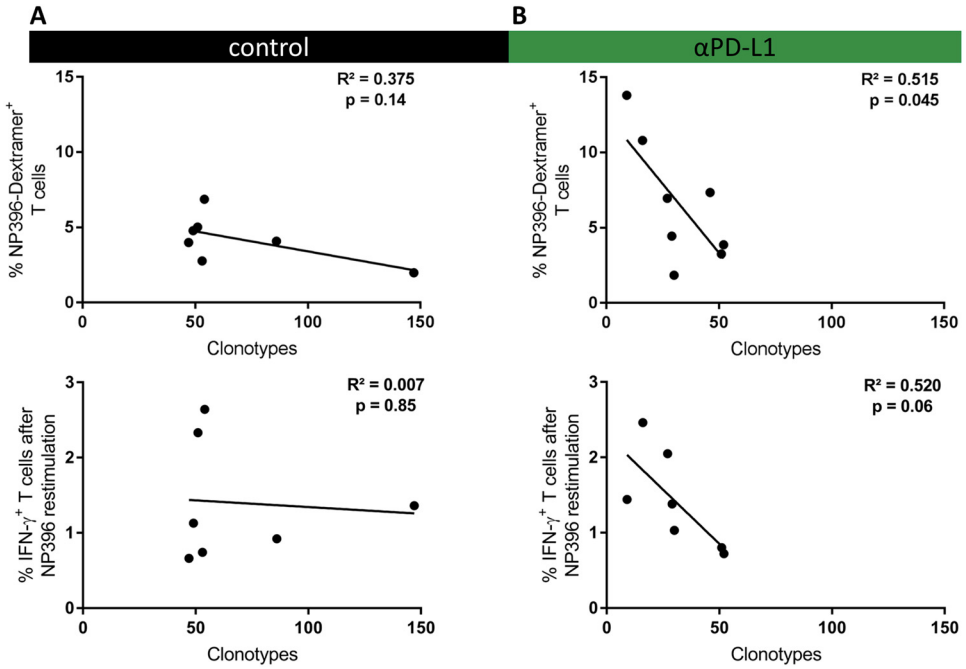

FIG 6 Treatment-induced negative correlation of TCR-β clonotypes and NP396-specific T cell response. NP396-specific TCR-β clonotype numbers from control-treated and anti-PD-L1-treated persistently LCMV cl13-infected mice were correlated with the respective physical and functional immune response for each individual mouse. The Dextramer-specific response of control-treated (A) and anti-PD-L1-treated (B) mice as well as the IFN-γ^+ responses of both groups are shown. Statistical correlation is depicted as linear regression with R^2 and P value within the respective graph. Results are pooled from 3 independent experiments.

test this hypothesis, we analyzed the NP396-specific CDR3 regions in regard to their motif similarities with a previously published program, tcrdist (42). Common motifs can be recognized by tcrdist, which may not appear due to random occurrence, in an antigen-specific TCR repertoire. Although we aimed to find a common motif in the hyperexpanded clonotypes, no common motif was detectable either in the different treatment groups or in all hyperexpanded clonotypes (data not shown). Another feature of tcrdist is biostatistical tree building, in which all clonotypes are ordered in regard to their CDR3 motif similarity. Each branch represents a single clonotype. Ten motifs are then biostatistically calculated, covering different branches of the tree. In order to increase our analytical depth, we expanded our sample set by using the four most dominant clonotypes of each mouse in the respective group, instead of only hyperexpanded clonotypes. This newly calculated clonotype repertoire represented the dominant immune responses and T cell specificities in chronic and anti-PD-L1-treated groups and was used to run the program tcrdist with this data set (Fig. 7). tcrdist generated two trees with our two data sets and calculated with 24 (control [Fig. 7A]) and 30 (anti-PD-L1 [Fig. 7B]) clonotypes, respectively. With the 10-motif calculation, only 13 of the 24 clonotypes were covered in control-treated mice (54%), whereas 21 of 30 clonotypes (70%) were covered in the anti-PD-L1-treated group. This was an indication that the clonotypes in our anti-PD-L1-treated mice were more similar to each other motif-wise than those in control mice. To confirm this, a nearest-neighbor analysis was performed with tcrdist. This calculates a biostatistical index of how closely related each clonotype is in relation to a certain number of other clonotypes. For example, the lower the "nearest neighbor 5" index is, the higher is the similarity of a clonotype to its five most similar neighbors within the repertoire. Calculating the average for our data sets the nearest neighbor 5 indices (67.0 for the control-treated group and 47.2 for the anti-PD-L1-treated group) as well as the nearest neighbor 10 indices (71.4 for the control-treated group and 55.7 for the anti-PD-L1-treated group) confirmed a higher

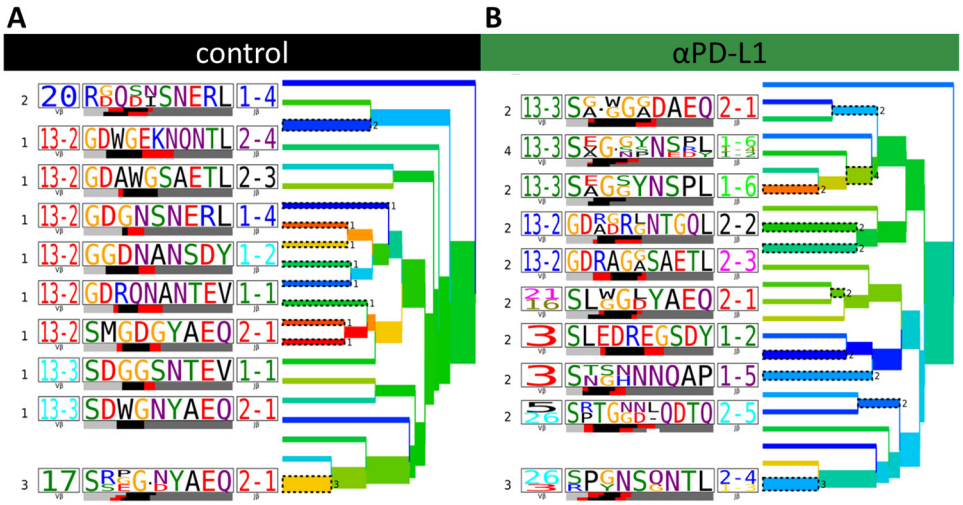

FIG 7 tcrdist revealed higher similarities of expanded clonotypes after anti-PD-L1 treatment. tcrdist analysis (42) of the four most abundant NP396-specific TCR-β clonotypes from all control-treated (A) and anti-PD-L1-treated (B) persistently LCMV cl13-infected C57BL/6 mice are depicted in relation to the CDR3 similarity: 10 motifs are selected by the tcrdist program to represent different branches of the similarity tree. Vβ chain, CDR3 amino acid sequence, and Jβ chain are depicted for each motif. Results are pooled from 3 independent experiments.

similarity of the CDR3 motifs from clonotypes of the TCR repertoires of the anti-PD-L1-treated mice than for the control-treated mice.

Our results showed that no common motif was detectable in the hyperexpanded clonotypes. However, the clonotypes of the TCR repertoires revealed more closely related CDR3 motifs after anti-PD-L1 treatment. This indicates that no single CDR3 motif is necessary for a T cell to hyperexpand, although a quite closely related range of motifs seems suitable to react to the epitope in a way that the T cell is triggered toward hyperexpansion by the anti-PD-L1 treatment.

DISCUSSION

Checkpoint inhibition has been implemented as a very successful treatment for certain cancer types, and some studies have been performed with patients with chronic viral infections (e.g., HBV and HCV) (8, 10). Although checkpoint inhibitors are a major breakthrough therapy for cancer, not all patients respond to treatment (43). Mechanisms that help to explain the different responses are insufficiently understood but could be important to optimize treatment and reduce potential side effects (24). One important question which still is poorly investigated is if checkpoint inhibitor treatment influences the diversity, hierarchy, and specificity of antigen-specific T cell responses. For this analysis, we used the well-established persistent LCMV infection model in C57BL/6 mice.

Our data could confirm physical and functional restoration of the antigen-specific CD8$^+$ T cell response by anti-PD-L1 therapy, as published by Barber et al. (6). With a focus on the strongly exhausted immune response against the LCMV epitope NP396, we revealed severe modulations of the TCR repertoire due to anti-PD-L1 therapy. While the number of NP396-specific T cells in our mice was increased due to anti-PD-L1 treatment (Fig. 1C), the TCR repertoire was focused to roughly half of the clonotypes compared to the TCR repertoire of control-treated mice (Fig. 2A). This could be explained by the appearance of single highly abundant (hyperexpanded) clonotypes and the subsequent reduction of detected rare clonotypes (Fig. 5). Although we could find neither a specific Vβ chain (Fig. 3) nor a certain CDR3 amino acid length which was used by these "reacting" clonotypes (Fig. 4), we could show certain patterns. We found only four TCR Vβ chains that were used in hyperexpanded clonotypes, and all of these clonotypes had CDR3 regions of either 14, 15, or 16 aa in length (Fig. 4). Comparison of the TCR repertoires has shown that the CDR3 length is modulated by their antigen

experience. Naive and naive-like memory T cells display a longer CDR3 length than do antigen-experienced effector T cells (39–41). Our findings of longer CDR3 length in NP396-specific T cells upon anti-PD-L1 blockade are in line with the findings that stem cell-like T cells respond to the anti-PD-L1 blockade (28). Motif analysis with tcrdist (Fig. 7) supported these results by revealing no common motif. However, the main clonotypes in anti-PD-L1-treated mice were clearly more similar to each other than were clonotypes from control mice. This is in line with findings in Epstein-Barr virus (EBV)-positive diffuse large B cell lymphoma (DLBCL) (44). It seems as if a few clonotypes of NP396-specific T cells were selected out of a pool of closely related ones that developed into hyperexpanded clonotypes. Thereby other responding clonotypes might have gotten lost, leading to a more oligoclonal TCR repertoire. This process seems to be efficient for clearing the virus, because it correlated with stronger LCMV-specific T cell responses (Fig. 6). That narrowing of the TCR repertoire can result in a better outcome has been shown in HIV infection and anti-PD-1-treated melanoma patients (32, 45). On the other hand, a narrowed, oligoclonal TCR repertoire is associated with immune evasion of viruses and also with disease progression, e.g., in DLBCL (44, 46, 47).

There are some limitations of this study. Due to limited number of NP396-specific T cells acquired from blood, only a snapshot of the TCR repertoire could be taken. Therefore, we could not analyze the TCR repertoire prior to, during, and after anti-PD-L1 treatment, which would give more insight into the individual changes of the TCR repertoire in each treated individual. Additionally, our investigations were focused on bulk TCR Vβ analysis, giving a representative overview of the TCR repertoire. A different approach is single-cell analysis. This would give information about TCR-α and -β chain pairings, to analyze TCR clonotypes more precisely. However, this method would analyze only a small number of T cells and make it hardly possible to recognize the hyperexpansion reported here. Besides the TCR, the phenotypic status of T cells is important to assess their restoration capacity: the current understanding is that only a small subpopulation of partially exhausted T cells, which still express, e.g., TCF-1, can be restored by checkpoint inhibition (26–28, 48). With our experimental setup we were not able to investigate the TCR repertoires of different NP396-specific T cell subpopulations, e.g., TCF-1$^+$, which would answer our hypothesis that the hyperexpanded clonotypes with the longer CDR3 regions are stem cell-like T cells.

To our knowledge, our study is the first one to investigate the effect of anti-PD-L1 blockade on the TCR repertoire in chronically LCMV-infected mice. Our study shows that the TCR repertoire is drastically narrowed in chronic versus LCMV immune mice, in which the NP396-specific TCR repertoire is even less diverse after checkpoint inhibitor treatment. These narrowed, oligoclonal, and private LCMV-specific responses are associated with higher T cell functionality. However, whether this narrowed and skewed response is beneficial or harmful for the host acquiring homologous and/or heterologous pathogen infection is still an important topic to investigate.

MATERIALS AND METHODS

Ethics statement. All mouse experiments were performed in accordance with the guidelines of Medical School Hannover (MHH), Germany, the national animal protection law (Tierschutzgesetz), and the animal experiment regulations (Tierschutz-Versuchstierverordnung). The study was approved by the State of Lower Saxony (LAVES—Niedersächsisches Landesamt für Verbraucherschutz und Lebensmittelsicherheit) under project number 33.12–42502-04-16/2127. The highest possible ethical standards were ensured, and all efforts were made to reduce suffering of the mice.

Mice and treatment. Male C57BL/6 mice, 6 to 8 weeks old, were bred under and kept under pathogen-free conditions, with a 12/12-h day/night cycle, in the general animal facility of MHH. For the LCMV mouse model, mice were infected intravenously with 2×10^6 PFU of LCMV cl13 to generate persistently LCMV-infected mice. In contrast to many published studies of LCMV-specific T cell restoration using anti-PD-L1, we did not used the deep-exhaustion LCMV mouse model, in which CD4 T cells are depleted prior to LCMV cl13 infection, which results in a more stable chronic LCMV infection (6, 25, 36). LCMV Armstrong (5×10^4 PFU) is cleared by C57BL/6 mice after an acute infection, and mice were considered to be immune 4 weeks postinfection (LCMV immune). Blood was collected 21 days postinfection via the vena facialis to determine the exhaustion status by assessing the dominant NP396-specific CD8$^+$ T cell response. Beginning at day 23 postinfection, mice were treated five times (every third day)

intraperitoneally with 200 μg of anti-PD-L1 (10F.9G2 [BioXcell and Biolegend]), 500 μg of anti-CTLA-4 (UC10-4F10-11 [BioXcell] and 9H10 [Biolegend]), or phosphate-buffered saline (PBS) as a control. At day 36 postinfection, mice were sacrificed and spleens and kidneys were harvested (Fig. 1A).

Virus titer determination. LCMV titers were determined by plaque assay as described before (34). Briefly, serial dilutions of log10s of kidney tissue homogenate were incubated on Vero cells with ~70% confluence in a 6-well plate. Staining was performed 4 days postinfection with neutral red (Sigma-Aldrich); 2 days later, plaques were counted and PFU per organ were calculated.

Synthetic peptide and Dextramer. The synthetic peptide $NP_{396-404}$ (FQPQNGQFI) was purchased from ProImmune. The Dextramer H-2D^b/FQPQNGQFI (NP396) was purchased from Immudex.

Cell surface and Dextramer staining for flow cytometry. Single-cell suspensions from spleens were treated with lysis buffer (155 mM NH_4Cl, 10 mM $KHCO_3$, and 1 mM EDTA [Sigma-Aldrich]) to remove red blood cells. Afterwards, $\geq 1 \times 10^6$ cells were FCγR blocked with anti-CD16/32 (2.4G2; BD Bioscience) and stained with anti-CD8α (53-6.7; Biolegend), anti-CD44 (IM7; Biolegend), viability stain (fixable viability stain 700; BD Bioscience), anti-PD-1 (29F.1A12; Biolegend), and Dextramer reagents (Immudex).

Intracellular cytokine measurement. Red blood cells were removed from single-cell suspensions from spleens (as described above). Splenocytes (1.5×10^6 per well) were stimulated in 200 μl of RPMI medium (Gibco) with 1 μg/ml of NP396 peptide and 0.2 μl of GolgiPlug (BD Bioscience). As a positive control, anti-CD3 antibody (145-2C11; eBioscience) was used, and as a negative control, medium was used. Cells were incubated for 4.5 h at 37°C and 5% CO_2. After incubation, surface stainings were performed (as described above). For intracellular staining, cells were permeabilized with the True-Nuclear transcription buffer set (Biolegend) according to the manufacturer's protocol. Furthermore, cells were stained in the included washing buffer with anti-IFN-γ (XMG1.2; Biolegend) and anti-TNF-α (Mp6-XT22; Biolegend). Flow cytometry was performed with a BD LSRFortessa (BD; 3 lasers and 14 colors).

Next-generation sequencing of the NP396-specific T cell receptor repertoire. TCR repertoire analyses were performed on NP396-specific CD8$^+$ T cells. Single-cell suspensions of spleens were stained with anti-CD8α (53-6.7; Biolegend), anti-CD4 (RM4-5; Biolegend), anti-CD44 (IM7; Biolegend), viability stain (fixable viability stain 700; BD Bioscience), and Dextramer NP396 (H2-D^b; Immudex). Fluorescence-activated cell sorting (FACS) was used to gain the CD4$^-$ CD8α^+ CD44$^+$ NP396$^+$ cell population. Cells were directly sorted into RLT buffer (RNeasy plus microRNA extraction kit; Qiagen) and stored at −80°C. According to the manufacturer's protocols, the sample was prepared as follows: for RNA extraction, the RNeasy kit was used, taking ~10,000 epitope-specific cells in 350 μl of RLT buffer (RNeasy plus microRNA extraction kit; Qiagen). RNA was instantly used to transcribe cDNA by performing a SMART RACE (rapid amplification of cDNA ends) PCR (SMARTer RACE cDNA amplification kit; Clontech). cDNA was further amplified using Illumina adapter-containing primers (5′-CTAATACGACTCACTATAGGGCAAGCAGTGGTAT CAACGCAGAGT-3′ and 5′-CTAATACGACTCACTATAG GGC-3′) as well as a TCR-β-specific primer (5′-TGG CTCAAACAAGGAGACCT-3′) within a second PCR (34 cycles) (Advantage 2PCR kit; Clontech). Amplicon size was determined by running an agarose gel (2% agarose in Tris-acetate-EDTA buffer containing ethidium bromide solution). Bands were cut out of the gel, and nucleotides were extracted (QIAquick gel extraction kit; Qiagen). Afterwards, samples were indexed by using 10 μM Nextera primer combinations (Illumina) in a 10-cycle PCR with the Advantage 2PCR kit (Clontech). The indexed amplicons were purified by adding 90 μl of AMPure XP beads (Beckman Coulter). After 5 min of incubation, the plate was placed on a magnetic plate. When the beads were mostly accumulated at the wall of the wells, all wells were washed with 70% ethanol. To elute the DNA from the beads, the beads were diluted in 100 μl of H_2O. Due to magnetic separation, DNA could be transferred into a new plate while the beads remained on the walls of the wells. Finally, all sample concentrations were determined with Quant-iT PicoGreen double-stranded DNA (dsDNA) assay kit (Thermo Fisher Scientific) and mixed to have an equal concentration of each sample in the final sequencing sample mixture. Sequencing was performed with a Miseq (Illumina) by using V2 chemistry and 150-bp paired-end sequencing.

Sequencing analysis. Quality control of forward and reverse reads for each individual sample was performed using fastp (49). Assembling and alignment of reads to certain TCR-β clonotypes were performed using MiXCR (50). Finally, the number of clonotypes was trimmed down by using a 96% cutoff, as described before (51), in order to avoid artificial diversity increases by erroneous sequences. Graphical depiction was done using R-based programs VDJtools (52) and ClonoPlot (53) as well as tcrdist (42).

Statistics. Descriptive statistics are expressed as means ± standard errors of the means. Depending on the standard deviation, Student's t tests, Mann-Whitney U tests, analysis of variance (ANOVA), or Kruskal-Wallis tests were performed, using Prism 7.03 software (GraphPad Software).

Data availability. All clonotypes of sequencing data are available online via the Repomed server at https://doi.org/10.26068/mhhrpm/20200609-003.

ACKNOWLEDGMENTS

This work was supported by a grant from the German Research Association (DFG) (KR 2913/2-1 to A.R.M.K.).

We have no competing interests to declare.

The Centre for Individualised Infection Medicine (CiiM) is a joint venture of the Helmholtz Centre for Infection Research and the Hannover Medical School, Hannover, Germany.

REFERENCES

1. Larkin J, Hatswell AJ, Nathan P, Lebmeier M, Lee D. 2015. The predicted impact of ipilimumab usage on survival in previously treated advanced or metastatic melanoma in the UK. PLoS One 10:e0145524. https://doi.org/10.1371/journal.pone.0145524.
2. Horn L, Gettinger SN, Gordon MS, Herbst RS, Gandhi L, Felip E, Sequist LV, Spigel DR, Antonia SJ, Balmanoukian A, Cassier PA, Liu B, Kowanetz M, O'Hear C, Fasso M, Grossman W, Sandler A, Soria JC. 2018. Safety and clinical activity of atezolizumab monotherapy in metastatic non-small-cell lung cancer: final results from a phase I study. Eur J Cancer 101:201–209. https://doi.org/10.1016/j.ejca.2018.06.031.
3. Rittmeyer A, Barlesi F, Waterkamp D, Park K, Ciardiello F, von Pawel J, Gadgeel SM, Hida T, Kowalski DM, Dols MC, Cortinovis DL, Leach J, Polikoff J, Barrios C, Kabbinavar F, Frontera OA, De Marinis F, Turna H, Lee JS, Ballinger M, Kowanetz M, He P, Chen DS, Sandler A, Gandara DR, OAK Study Group. 2017. Atezolizumab versus docetaxel in patients with previously treated non-small-cell lung cancer (OAK): a phase 3, open-label, multicentre randomised controlled trial. Lancet 389:255–265. https://doi.org/10.1016/S0140-6736(16)32517-X.
4. Robert L, Tsoi J, Wang X, Emerson R, Homet B, Chodon T, Mok S, Huang RR, Cochran AJ, Comin-Anduix B, Koya RC, Graeber TG, Robins H, Ribas A. 2014. CTLA4 blockade broadens the peripheral T-cell receptor repertoire. Clin Cancer Res 20:2424–2432. https://doi.org/10.1158/1078-0432.CCR-13-2648.
5. Topalian SL, Wolchok JD, Chan TA, Mellman I, Palucka K, Banchereau J, Rosenberg SA, Dane Wittrup K. 2015. Immunotherapy: the path to win the war on cancer? Cell 161:185–186. https://doi.org/10.1016/j.cell.2015.03.045.
6. Barber DL, Wherry EJ, Masopust D, Zhu B, Allison JP, Sharpe AH, Freeman GJ, Ahmed R. 2006. Restoring function in exhausted CD8 T cells during chronic viral infection. Nature 439:682–687. https://doi.org/10.1038/nature04444.
7. Bengsch B, Martin B, Thimme R. 2014. Restoration of HBV-specific CD8+ T cell function by PD-1 blockade in inactive carrier patients is linked to T cell differentiation. J Hepatol 61:1212–1219. https://doi.org/10.1016/j.jhep.2014.07.005.
8. Fisicaro P, Valdatta C, Massari M, Loggi E, Biasini E, Sacchelli L, Cavallo MC, Silini EM, Andreone P, Missale G, Ferrari C. 2010. Antiviral intrahepatic T-cell responses can be restored by blocking programmed death-1 pathway in chronic hepatitis B. Gastroenterology 138:682–684. https://doi.org/10.1053/j.gastro.2009.09.052.
9. Rinker F, Zimmer CL, Höner Zu Siederdissen C, Manns MP, Kraft ARM, Wedemeyer H, Björkström NK, Cornberg M. 2018. Hepatitis B virus-specific T cell responses after stopping nucleos(t)ide analogue therapy in HBeAg-negative chronic hepatitis B. J Hepatol 69:584–593. https://doi.org/10.1016/j.jhep.2018.05.004.
10. Urbani S, Amadei B, Tola D, Pedrazzi G, Sacchelli L, Cavallo MC, Orlandini A, Missale G, Ferrari C. 2008. Restoration of HCV-specific T cell functions by PD-1/PD-L1 blockade in HCV infection: effect of viremia levels and antiviral treatment. J Hepatol 48:548–558. https://doi.org/10.1016/j.jhep.2007.12.014.
11. Wykes MN, Lewin SR. 2018. Immune checkpoint blockade in infectious diseases. Nat Rev Immunol 18:91–104. https://doi.org/10.1038/nri.2017.112.
12. Owusu Sekyere S, Suneetha PV, Kraft AR, Zhang S, Dietz J, Sarrazin C, Manns MP, Schlaphoff V, Cornberg M, Wedemeyer H. 2015. A heterogeneous hierarchy of co-regulatory receptors regulates exhaustion of HCV-specific CD8 T cells in patients with chronic hepatitis C. J Hepatol 62:31–40. https://doi.org/10.1016/j.jhep.2014.08.008.
13. Velu V, Titanji K, Zhu B, Husain S, Pladevega A, Lai L, Vanderford TH, Chennareddi L, Silvestri G, Freeman GJ, Ahmed R, Amara RR. 2009. Enhancing SIV-specific immunity in vivo by PD-1 blockade. Nature 458:206–210. https://doi.org/10.1038/nature07662.
14. Davar D, Wilson M, Pruckner C, Kirkwood JM. 2015. PD-1 blockade in advanced melanoma in patients with hepatitis C and/or HIV. Case Rep Oncol Med 2015:737389. https://doi.org/10.1155/2015/737389.
15. Sangro B, Gomez-Martin C, de la Mata M, Iñarrairaegui M, Garralda E, Barrera P, Riezu-Boj JI, Larrea E, Alfaro C, Sarobe P, Lasarte JJ, Pérez-Gracia JL, Melero I, Prieto J. 2013. A clinical trial of CTLA-4 blockade with tremelimumab in patients with hepatocellular carcinoma and chronic hepatitis C. J Hepatol 59:81–88. https://doi.org/10.1016/j.jhep.2013.02.022.
16. Wherry EJ, Kurachi M. 2015. Molecular and cellular insights into T cell exhaustion. Nat Rev Immunol 15:486–499. https://doi.org/10.1038/nri3862.
17. Zajac AJ, Blattman JN, Murali-Krishna K, Sourdive DJ, Suresh M, Altman JD, Ahmed R. 1998. Viral immune evasion due to persistence of activated T cells without effector function. J Exp Med 188:2205–2213. https://doi.org/10.1084/jem.188.12.2205.
18. Wherry EJ, Ahmed R. 2004. Memory CD8 T-cell differentiation during viral infection. J Virol 78:5535–5545. https://doi.org/10.1128/JVI.78.11.5535-5545.2004.
19. Blackburn SD, Shin H, Haining WN, Zou T, Workman CJ, Polley A, Betts MR, Freeman GJ, Vignali DA, Wherry EJ. 2009. Coregulation of CD8+ T cell exhaustion by multiple inhibitory receptors during chronic viral infection. Nat Immunol 10:29–37. https://doi.org/10.1038/ni.1679.
20. Brown JA, Dorfman DM, Ma FR, Sullivan EL, Munoz O, Wood CR, Greenfield EA, Freeman GJ. 2003. Blockade of programmed death-1 ligands on dendritic cells enhances T cell activation and cytokine production. J Immunol 170:1257–1266. https://doi.org/10.4049/jimmunol.170.3.1257.
21. Freeman GJ, Wherry EJ, Ahmed R, Sharpe AH. 2006. Reinvigorating exhausted HIV-specific T cells via PD-1-PD-1 ligand blockade. J Exp Med 203:2223–2227. https://doi.org/10.1084/jem.20061800.
22. Nakamoto N, Kaplan DE, Coleclough J, Li Y, Valiga ME, Kaminski M, Shaked A, Olthoff K, Gostick E, Price DA, Freeman GJ, Wherry EJ, Chang KM. 2008. Functional restoration of HCV-specific CD8 T cells by PD-1 blockade is defined by PD-1 expression and compartmentalization. Gastroenterology 134:1927–1922. https://doi.org/10.1053/j.gastro.2008.02.033.
23. Jin HT, Anderson AC, Tan WG, West EE, Ha SJ, Araki K, Freeman GJ, Kuchroo VK, Ahmed R. 2010. Cooperation of Tim-3 and PD-1 in CD8 T-cell exhaustion during chronic viral infection. Proc Natl Acad Sci U S A 107:14733–14738. https://doi.org/10.1073/pnas.1009731107.
24. Heinzerling L, de Toni EN, Schett G, Hundorfean G, Zimmer L. 2019. Checkpoint inhibitors. Dtsch Arztebl Int 116:119–126. https://doi.org/10.3238/arztebl.2019.0119.
25. Snell LM, MacLeod BL, Law JC, Osokine I, Elsaesser HJ, Hezaveh K, Dickson RJ, Gavin MA, Guidos CJ, McGaha TL, Brooks DG. 2018. CD8(+) T cell priming in established chronic viral infection preferentially directs differentiation of memory-like cells for sustained immunity. Immunity 49:678–694.e5. https://doi.org/10.1016/j.immuni.2018.08.002.
26. Siddiqui I, Schaeuble K, Chennupati V, Fuertes Marraco SA, Calderon-Copete S, Pais Ferreira D, Carmona SJ, Scarpellino L, Gfeller D, Pradervand S, Luther SA, Speiser DE, Held W. 2019. Intratumoral Tcf1(+)PD-1(+)CD8(+) T cells with stem-like properties promote tumor control in response to vaccination and checkpoint blockade immunotherapy. Immunity 50:195–211.e10. https://doi.org/10.1016/j.immuni.2018.12.021.
27. Buggert M, Tauriainen J, Yamamoto T, Frederiksen J, Ivarsson MA, Michaelsson J, Lund O, Hejdeman B, Jansson M, Sonnerborg A, Koup RA, Betts MR, Karlsson AC. 2014. T-bet and Eomes are differentially linked to the exhausted phenotype of CD8+ T cells in HIV infection. PLoS Pathog 10:e1004251. https://doi.org/10.1371/journal.ppat.1004251.
28. Im SJ, Hashimoto M, Gerner MY, Lee J, Kissick HT, Burger MC, Shan Q, Hale JS, Lee J, Nasti TH, Sharpe AH, Freeman GJ, Germain RN, Nakaya HI, Xue HH, Ahmed R. 2016. Defining CD8+ T cells that provide the proliferative burst after PD-1 therapy. Nature 537:417–421. https://doi.org/10.1038/nature19330.
29. Jadhav RR, Im SJ, Hu B, Hashimoto M, Li P, Lin JX, Leonard WJ, Greenleaf WJ, Ahmed R, Goronzy JJ. 2019. Epigenetic signature of PD-1+ TCF1+ CD8 T cells that act as resource cells during chronic viral infection and respond to PD-1 blockade. Proc Natl Acad Sci U S A 116:14113–14118. https://doi.org/10.1073/pnas.1903520116.
30. Cha E, Klinger M, Hou Y, Cummings C, Ribas A, Faham M, Fong L. 2014. Improved survival with T cell clonotype stability after anti-CTLA-4 treatment in cancer patients. Sci Transl Med 6:238ra70. https://doi.org/10.1126/scitranslmed.3008211.
31. Kvistborg P, Philips D, Kelderman S, Hageman L, Ottensmeier C, Joseph-Pietras D, Welters MJP, van der Burg S, Kapiteijn E, Michielin O, Romano E, Linnemann C, Speiser D, Blank C, Haanen JB, Schumacher TN. 2014. Anti-CTLA-4 therapy broadens the melanoma-reactive CD8(+) T cell response. Sci Transl Med 6:254ra128. https://doi.org/10.1126/scitranslmed.3008918.
32. Tumeh PC, Harview CL, Yearley JH, Shintaku IP, Taylor EJ, Robert L, Chmielowski B, Spasic M, Henry G, Ciobanu V, West AN, Carmona M,

Kivork C, Seja E, Cherry G, Gutierrez AJ, Grogan TR, Mateus C, Tomasic G, Glaspy JA, Emerson RO, Robins H, Pierce RH, Elashoff DA, Robert C, Ribas A. 2014. PD-1 blockade induces responses by inhibiting adaptive immune resistance. Nature 515:568–571. https://doi.org/10.1038/nature13954.
33. Rudqvist NP, Pilones KA, Lhuillier C, Wennerberg E, Sidhom JW, Emerson RO, Robins HS, Schneck J, Formenti SC, Demaria S. 2018. Radiotherapy and CTLA-4 blockade shape the TCR repertoire of tumor-infiltrating T cells. Cancer Immunol Res 6:139–150. https://doi.org/10.1158/2326-6066.CIR-17-0134.
34. Welsh RM, Seedhom MO. 2008. Lymphocytic choriomeningitis virus (LCMV): propagation, quantitation, and storage. Curr Protoc Microbiol Chapter 15:Unit 15A.1.
35. Zehn D, Wherry EJ. 2015. Immune memory and exhaustion: clinically relevant lessons from the LCMV model. Adv Exp Med Biol 850:137–152. https://doi.org/10.1007/978-3-319-15774-0_10.
36. Wherry EJ, Blattman JN, Murali-Krishna K, van der Most R, Ahmed R. 2003. Viral persistence alters CD8 T-cell immunodominance and tissue distribution and results in distinct stages of functional impairment. J Virol 77:4911–4927. https://doi.org/10.1128/jvi.77.8.4911-4927.2003.
37. Wang XZ, Stepp SE, Brehm MA, Chen HD, Selin LK, Welsh RM. 2003. Virus-specific CD8 T cells in peripheral tissues are more resistant to apoptosis than those in lymphoid organs. Immunity 18:631–642. https://doi.org/10.1016/S1074-7613(03)00116-X.
38. Kim SK, Cornberg M, Wang XZ, Chen HD, Selin LK, Welsh RM. 2005. Private specificities of CD8 T cell responses control patterns of heterologous immunity. J Exp Med 201:523–533. https://doi.org/10.1084/jem.20041337.
39. Kou ZC, Puhr JS, Wu SS, Goodenow MM, Sleasman JW. 2003. Combination antiretroviral therapy results in a rapid increase in T cell receptor variable region beta repertoire diversity within CD45RA CD8 T cells in human immunodeficiency virus-infected children. J Infect Dis 187:385–397. https://doi.org/10.1086/367674.
40. Hou X, Zeng P, Zhang X, Chen J, Liang Y, Yang J, Yang Y, Liu X, Diao H. 2019. Shorter TCR beta-chains are highly enriched during thymic selection and antigen-driven selection. Front Immunol 10:299. https://doi.org/10.3389/fimmu.2019.00299.
41. Afik S, Yates KB, Bi K, Darko S, Godec J, Gerdemann U, Swadling L, Douek DC, Klenerman P, Barnes EJ, Sharpe AH, Haining WN, Yosef N. 2017. Targeted reconstruction of T cell receptor sequence from single cell RNA-seq links CDR3 length to T cell differentiation state. Nucleic Acids Res 45:e148. https://doi.org/10.1093/nar/gkx615.
42. Dash P, Fiore-Gartland AJ, Hertz T, Wang GC, Sharma S, Souquette A, Crawford JC, Clemens EB, Nguyen THO, Kedzierska K, La Gruta NL, Bradley P, Thomas PG. 2017. Quantifiable predictive features define epitope-specific T cell receptor repertoires. Nature 547:89–93. https://doi.org/10.1038/nature22383.
43. Nishijima TF, Muss HB, Shachar SS, Moschos SJ. 2016. Comparison of efficacy of immune checkpoint inhibitors (ICIs) between younger and older patients: a systematic review and meta-analysis. Cancer Treat Rev 45:30–37. https://doi.org/10.1016/j.ctrv.2016.02.006.
44. Keane C, Gould C, Jones K, Hamm D, Talaulikar D, Ellis J, Vari F, Birch S, Han E, Wood P, Le-Cao KA, Green MR, Crooks P, Jain S, Tobin J, Steptoe RJ, Gandhi MK. 2017. The T-cell receptor repertoire influences the tumor microenvironment and is associated with survival in aggressive B-cell lymphoma. Clin Cancer Res 23:1820–1828. https://doi.org/10.1158/1078-0432.CCR-16-1576.
45. Conrad JA, Ramalingam RK, Duncan CB, Smith RM, Wei J, Barnett L, Simons BC, Lorey SL, Kalams SA. 2012. Antiretroviral therapy reduces the magnitude and T cell receptor repertoire diversity of HIV-specific T cell responses without changing T cell clonotype dominance. J Virol 86:4213–4221. https://doi.org/10.1128/JVI.06000-11.
46. Meyer-Olson D, Shoukry NH, Brady KW, Kim H, Olson DP, Hartman K, Shintani AK, Walker CM, Kalams SA. 2004. Limited T cell receptor diversity of HCV-specific T cell responses is associated with CTL escape. J Exp Med 200:307–319. https://doi.org/10.1084/jem.20040638.
47. Cornberg M, Chen AT, Wilkinson LA, Brehm MA, Kim SK, Calcagno C, Ghersi D, Puzone R, Celada F, Welsh RM, Selin LK. 2006. Narrowed TCR repertoire and viral escape as a consequence of heterologous immunity. J Clin Invest 116:1443–1456. https://doi.org/10.1172/JCI27804.
48. Kratchmarov R, Magun AM, Reiner SL. 2018. TCF1 expression marks self-renewing human CD8(+) T cells. Blood Adv 2:1685–1690. https://doi.org/10.1182/bloodadvances.2018016279.
49. Chen S, Zhou Y, Chen Y, Gu J. 2018. fastp: an ultra-fast all-in-one FASTQ preprocessor. Bioinformatics 34:i884–i890. https://doi.org/10.1093/bioinformatics/bty560.
50. Bolotin DA, Poslavsky S, Mitrophanov I, Shugay M, Mamedov IZ, Putintseva EV, Chudakov DM. 2015. MiXCR: software for comprehensive adaptive immunity profiling. Nat Methods 12:380–381. https://doi.org/10.1038/nmeth.3364.
51. Warren RL, Freeman JD, Zeng T, Choe G, Munro S, Moore R, Webb JR, Holt RA. 2011. Exhaustive T-cell repertoire sequencing of human peripheral blood samples reveals signatures of antigen selection and a directly measured repertoire size of at least 1 million clonotypes. Genome Res 21:790–797. https://doi.org/10.1101/gr.115428.110.
52. Shugay M, Bagaev DV, Turchaninova MA, Bolotin DA, Britanova OV, Putintseva EV, Pogorelyy MV, Nazarov VI, Zvyagin IV, Kirgizova VI, Kirgizov KI, Skorobogatova EV, Chudakov DM. 2015. VDJtools: unifying post-analysis of T cell receptor repertoires. PLoS Comput Biol 11:e1004503. https://doi.org/10.1371/journal.pcbi.1004503.
53. Fahnrich A, Krebbel M, Decker N, Leucker M, Lange FD, Kalies K, Moller S. 2017. ClonoCalc and ClonoPlot: immune repertoire analysis from raw files to publication figures with graphical user interface. BMC Bioinformatics 18:164. https://doi.org/10.1186/s12859-017-1575-2.